

State of Oregon
Department of Geology and Mineral Industries
910 State Office Building
1400 SW Fifth Avenue
Portland, Oregon 97201

OPEN-FILE REPORT O-89-08

SUBMERSIBLE OBSERVATIONS AND BOTTOM-SAMPLE ANALYSES
OF THE SEA CLIFF HYDROTHERMAL FIELD, GORDA RIDGE

by

James S. McClain
and
Peter Schiffman
Department of Geology
University of California, Davis

Final Report for Contract No. 63-630-8804

Submitted to:

Oregon Department of Geology and Mineral Industries
and the
Gorda Ridge Technical Task Force

Released March 1989

NOTICE

This report is based on results of a research program directed by the joint federal-state Gorda Ridge Technical Task Force, managed by the Oregon Department of Geology and Mineral Industries, and funded by the Minerals Management Service, U.S. Department of the Interior, through Cooperative Agreement. Opinions expressed are those of the authors and do not constitute endorsement by the sponsoring agencies or the Task Force.

The Oregon Department of Geology and Mineral Industries is publishing this paper because the subject matter is consistent with the mission of the Department. To facilitate timely distribution of information, camera-ready copy submitted by the authors has not been edited by the staff of the Oregon Department of Geology and Mineral Industries.

CONTENTS

ABSTRACT	1
INTRODUCTION	2
The Northern Gorda Ridge	2
SUBMERSIBLE OBSERVATIONS	4
Summary	5
Analysis of sample	7
Analytical techniques	7
Hydrothermal crusts	7
Chimney fragments	8
Basalt fragment	8
Mineral chemistry	9
DISCUSSION	9
CONCLUSIONS	11
REFERENCES	12
FIGURE CAPTIONS	13

ILLUSTRATIONS

Figures

1a. Geologic map	14
1b. Sample location map	15
2. Photographs of hydrothermal crust and chimney samples	16
3. X-ray diffraction powder pattern of crust sample	17
4. Backscattered electron micrographs of crust and chimney samples	18
5. Qualitative XRF analyses of crust sample 769-1:	
a. by direct excitation	19
b. with a Ge secondary fluorescence target	20
c. with a Rh fluorescence target	21
6. Electron microprobe analysis of layer silicates	22
7. Diagram showing Sr versus Ba contents of barites	23

Tables

1. List and description of samples	24
2. Analyses of layer silicates	25
3. Analyses of sulfides	26
4. Analyses of sulfates	27

ABSTRACT

As part of the 1988 Gorda Ridge Technical Task Force project, we undertook a program of submersible observations and bottom sample analysis of a hydrothermal field discovered on the walls of the rift valley of the northern Gorda Ridge. The presence of the field, known as the Sea Cliff Hydrothermal Field, largely confirms the hypothesis that faults accommodate fluid flow on mid-ocean ridges and control the distribution of vents.

The hydrothermal field is characterized by a broad region of diffuse venting though basalt talus and cliffs, by an area of hydrothermal breccia crust overlying sediments, and by a small area of extremely active vents.

The hydrothermal crust is a breccia comprising an indurated but porous siliceous material. The breccia is composed of angular to rounded, black, grey, or white colored clasts enclosed in a dark grey, porous matrix. Pore spaces are typically ingrown with barite. Many silica clasts contain small sulfide (dominantly pyrite/marcasite, with chalcopyrite) inclusions. The matrix is composed of amorphous silica, with barite, and disseminated clots of sulfide (dominantly marcasite, pyrite and chalcopyrite, and rarer sphalerite).

The vent chimneys were found to be emitting waters with temperatures of up to 248°C. The high temperature fluids were clear to grey in color; no "black smokers" were observed. The chimneys were found to be extremely soft, and they would crumble on contact. Despite this, samples from the chimney were recovered. One fragment was texturally and mineralogically similar to the crust samples. A second chimney fragment was quite distinct, composed of anhydrite, locally rimmed by fibrous aggregates of Mg-silicate. Some sphalerite was also observed.

While the Sea Cliff Hydrothermal Field has only just been discovered, and much more work needs to be done, we have established the importance of the rift valley wall faults for hydrothermal circulation. The full extent of this field, in particular the total volume of hydrothermal material, is not yet known, although it may not be large. However, future minerals exploration should include reconnaissance work on the rift valley walls as well as at the center of the rift valley.

Introduction

With the discovery of high temperature hydrothermal vents on the mid-ocean ridges came dramatic confirmation of the importance of hydrothermal circulation to the thermal and chemical budgets of the oceanic lithosphere. As the number of observations of vents increases, many fundamental and important questions remain. One of the most important is that of the longevity, or persistence of a typical vent or vent field. The contribution of the field to the cooling of the lithosphere and the size of resulting hydrothermal deposits all depend on how long the vents continue to be active.

This longevity of a vent field is tied to the size (volume) and nature of the sources supplying heat to the circulating water. Early workers presumed that the sources were magma chambers thought to exist beneath the mid-ocean ridges. Indeed, most of the early observations of "black smokers" occurred along the faster spreading ridge segments where magma was thought to be plentiful. Slower spreading ridge segments, with rift valleys did not have active vents.

More recent observations contradict the link between magma chambers and high temperature vents. The highest temperature vents occur along the Endeavour Segment of the Juan de Fuca Ridge where seismic experiments have failed to identify any evidence for a magma chamber. Furthermore, the largest sulfide deposits known occur on the TAG field on the Mid-Atlantic Ridge where a magma chamber, if any, should be small and ephemeral. What many of these fields have in common is that they lie along faulted and/or fissured portions of the ridge, rather than along the younger axial region. This suggests that the distribution and longevity of vents is controlled more by the presence of faults than the size of the underlying magma chamber. It is possible that even in the absence of magma, deep penetrating faults may provide a conduit for water to interact with greater volumes of hot (albeit, not melted) rock, resulting in long-lived vents or vent fields.

The above hypothesis has practical applications for the future of minerals exploration on the mid-ocean ridges, for it implies that the best place to look for larger deposits may be along faults, rather than in the neovolcanic zone (if any). Furthermore, the hypothesis suggests that rifted ridge segments, with faults penetrating perhaps into the mantle, may be better candidates for economic deposits.

Our proposal to the Gorda Ridge Technical Task Force was to test the hypothesis that hydrothermal vents may be accommodated and controlled by faults. Specifically, we proposed to examine the walls of the rift valley for evidence of vents, and to characterize those vents through submersible observations and the analysis of samples recovered from the walls.

The northern Gorda Ridge

Our project became part of the 1988 dive program on the northern Gorda Ridge. Several years of reconnaissance work aimed at assessing the potential mineral resources of the Gorda Ridge showed that sulfide deposition did occur in the Escanaba Trough on the southern part of the ridge, but much of the northern part was considered to be unlikely to have much venting. The ridge appears to be deficient in magma supply, with a well-developed rift valley and no evidence for an axial magma chamber. However, preliminary water column studies revealed temperature and

chemical anomalies consistent with hydrothermal venting. One area of the northern Gorda Ridge, known as GR-14, appeared particularly promising. On the basis of Sea MARK imagery, it was noted that beneath one water column anomaly there was an area where the rift valley walls (faults) intersected another structural trend (as yet unidentified, but probably a zone of faulting and fissuring). Perhaps the intersection of two sets of faults brought about a significant increase in permeability and resulted in vigorous hydrothermal venting (Rona and Clague, 1989).

On the basis of these observations the 1988 dive program was planned. Several dives were planned for the rift valley walls, and several for the valley floor where some hydrothermally altered rocks had been dredged. The U. C. Davis proposal and this report are concerned with the former, the attempt to discover venting on the rift valley wall.

Submersible Observations (dives 767,768,769)

The northern Gorda Ridge cruise departed from Eureka, California on September 17 and returned to port on October 1. Aboard were scientists from NOAA, the U.S.G.S., the University of Hawaii, Oregon State University, and University of California, at Davis. James McClain was the representative from the latter. The ship used was the Laney Chouest, a M.C.S. contract ship that serves as the tender for the U.S. Navy Deep Submergence Vehicle SEA CLIFF.

Due to bad weather, only three dives were completed on the rift valley walls. They were:

1. Dive 767. P. Rona (NOAA) and M. Fisk (OSU), observers.
2. Dive 768. G. Taghon (OSU) and R. Denlinger (U.S.G.S.), observers.
3. Dive 769. J. McClain (U.C.D.) and J. Wiltshire (U. of H.).

In addition, two other dives (not described here) took place on the rift valley floor.

The initial dive, 767, took place on September 23. During the dive it was discovered that the acoustic navigation was inoperable at the seafloor, probably because of the rough topography. In addition, it was later found that the depth gauge aboard the submersible occasionally gave inconsistent readings. These problems do not permit us to provide absolute locations for the observations. However, each dive was able to locate the vent field, and the relative locations of various features appear to be correct. As a part of the U.C.D. contribution to the project, we produced the map of the Sea Cliff hydrothermal field.

Dive 767 proceeded along the rift valley walls at a depth of 2750 meters (although this has been amended to 2710 meters based on other observations (see Figure 1). The walls were found to be scalloped with sediment filled gullies and rocky ridges. Substantial basalt talus was also observed, as were segments of steep walls exposing truncated pillow basalts. The character of the sediments appeared to change, becoming darker and more coarse grained as the submersible proceeded south. Evidence for minor hydrothermal venting was observed, including tube worms and stained rocks. The hydrothermal area was restricted in length, perhaps only a few tens of meters long, without any evidence for high temperatures.

Continuing south, the DSV Sea Cliff came upon an area of more active hydrothermal venting. Most prominent among the initial observations was the presence of tubeworm mounds 1 to 2 meters high and 5 meters in diameter. The mound was located on a rocky slope with much basalt talus. Thermally induced shimmering water could be seen emanating from many places along the rock wall.

After rising in the water column to get a location, the Sea Cliff set down on an area with a brown to orange crust that appeared to be hydrothermal material. A sample of the crust was taken (sample 767-3). Under the crust was coarse-grained sediment that was apparently quite hot, suggesting that the entire region was underlain by hydrothermal fluids. Proceeding northeast (see Figure 1), the submersible came upon a large an active chimney, with vigorous fluid venting. Attempts to sample the vents, and obtain a temperature failed and the dive had to be terminated.

Dive 768 took place on September 24, 1988. The dive approached the now-identified hydrothermal field from the west. Starting lower on the rift valley wall, the divers came upon a field of fossil (inactive) chimneys located on a well sedimented terrace (see Figure 1). An attempt to sample one of these chimneys was made. The chimney was knocked down, and as the submersible backed away, the chimney rebounded back to a nearly upright position. Unfortunately the dust kicked up by the submersible did not permit another attempt at sample taking. In fact, the fossil chimney field could not be found.

Later in the dive the submersible encounters many of the same features seen on the previous dive, with talus intruded by tube worms and shimmering water. Vigorous hydrothermal venting from prominent chimneys also were observed. The chimneys are white with black or purple splotches. The divers reported them as "black smokers" (the later dive and videos would suggest this is incorrect). Attempts to film, sample and measure the temperatures of the vents failed as the dive had to be terminated.

Dive 769 took place on September 26. Because the earlier two dives had failed to sample the active vents and accurately measure their temperatures, the goals of the third (and ultimately the last) dive were to survey the field systematically and to take samples.

Our initial sample (769-1) was a piece of the hydrothermal crust observed to cover much of the vent field. The crust was about 10 cm thick and covered a layer of sediments that were apparently very hot. The crust was devoid of tube worms or other biota, perhaps because the crust did not provide a firm enough substrate.

After traversing the area of hydrothermal crust at a depth of 2746 to 2740 meters we entered an area of basalt outcrops and talus. Here, we observed shimmering water and tube worms. No chimneys were seen. Further south the slope steepens and we left the hydrothermal area. We then rose to 2720 meters on the rift valley wall and begin traversing north back into the hydrothermal zone. At this depth the crust is not apparent and we see tube worms, stained rock (an indication of hydrothermal precipitation) and shimmering water. We collect a sample of basalt talus (769-2) and proceed north and upslope.

At a depth of 2711 meters, and at a location roughly corresponding with the vents seen in the earlier dives, we discover active vents with a large chimney standing as much as 2 meters high. The slope is about 20°, but increases below the chimney. The entire chimney was emitting water, and at several points the venting was particularly impressive. Close examination revealed that the water is not black, but rather grey, indicating that the vents may be slightly lower temperature. We measured the most vigorous flow and found a temperature of 248°C. We are able to obtain a sample of the chimney by scooping it with a coffee can (samples, 769-3). The chimney is extremely soft and friable; a portion disappears into a cloud of dust upon sampling. This is in marked contrast to the fossil chimneys observed on dive 768.

Northwest of the "grey smokers" we entered a zone of basalt outcrops and talus fields. Shimmering water was emitted over a broad region and large clumps of tube worms were observed.

Summary of submersible observations on the Sea Cliff field

The "Sea Cliff Hydrothermal Field" is located on the walls of the rift valley of the northern Gorda Ridge. It lies at depths between 2675 and 2800 meters, some 300

meters above the rift valley floor. It is therefore on the bounding fault of the rift valley. It is not clear if the fault provides a conduit for water circulation, if the fault has dissected into a hydrothermal aquifer, or if the cross-cutting structures noted from earlier high-resolution bathymetric imaging increase the permeability to allow the field to form.

The hydrothermal field extends over area of 400 by 300 meters or more. Much of it is characterized by diffuse venting through basalt talus and outcrops. In these areas little, if any, mineral deposition is present.

Thy Sea Cliff field displayed a rather broad region of hydrothermal "crust". The crust covers a layer of hydrothermally derived sediments. Sulfides are incorporated in the crust and probably the underlying sediments. It is not possible to calculate the total volume of these sediments, as their thickness is not yet known, but it could be substantial.

The most active vents within the hydrothermal field are associated with chimneys, probably predominantly barite and amorphous silica. These vents have intermediate temperatures (up to 248°C), and the water is grey in color upon precipitation of the minerals. The chimney field is not extensive. However, at least one fossil field is observed. It is reasonable to expect that further fossil chimneys (and perhaps active ones) lie near the presently mapped area.

From a scientific viewpoint, the observations made during the 1988 dive program support the hypothesis that faults control or accommodate hydrothermal circulation. On the Gorda Ridge, faults may be more important than the presence of magma in creating mineralizing vents. Furthermore, these observations suggest that further exploration along the rift valley walls is warranted.

Analysis of sample from the Sea Cliff Hydrothermal Field

Five samples, collected during GR-14-Sea Cliff-88 dives 767, 768, and 769 were analyzed by a variety of techniques to characterize their mineralogy and chemical composition. The samples include two hydrothermal crusts (767-3 and 769-1), two chimney fragments from a greysmoker spire (769-3), and a basalt fragment from within the active vent field (768-3). The location of the samples within the Sea Cliff hydrothermal field is shown on figure 1.

Analytical techniques: Slabs or splits of the five samples were obtained with a rock saw at the facilities of the U.S. Geological Survey in Menlo Park, California. Photos of four of these split sample are shown in figure 2. Because the hydrothermal samples are generally friable, they were impregnated in petro-epoxy to indurate them. Polished thin sections were prepared from all five samples for petrographic, scanning electron microscope (SEM), and electron microprobe (EM) analysis. SEM analysis was done using an Hitachi S-450 equipped with a Tracor Northern 2000 X-ray detector and G & W backscattered electron detector. EM analyses were conducted on a Cameca SX-50 probe operated at 15 KeV and 10 NA beam current. Pieces of the hydrothermal crust samples were powdered in a tungsten carbide shatter box for X-ray diffraction (XRD) and X-ray fluorescence (XRF) analyses. XRD analysis was conducted on a Phillips diffractometer, using Cu Ka X-radiation and a graphite monochromator. XRF analyses were obtained on a Kevex 700/8000 EDS system using both primary and secondary fluorescence techniques. All the above described analytical facilities are in the Dept. of Geology at U.C. Davis.

Hydrothermal crusts: Two samples, 767-3 and 769-1, are pieces of an indurated, but porous, siliceous material which forms a crust within the active vent field. Photos of slabbed crust samples are shown in figure 2 (a and b). The crusts are fragmental or clastic and are composed of angular to rounded, black, grey, or white colored clasts (< 2 cm, but commonly << 0.5 cm, in maximum dimension), enclosed in a dark grey, fine grained, porous matrix. Individual pores are generally less than 2 mm in diameter, but some approach 1 cm in maximum dimension. The pore spaces are typically ingrown with acicular, white crystals of barite, less than 1 mm in length.

The white, grey, and black clasts are dominantly composed of amorphous silica. An XRD powder pattern of this material (figure 3) displays a single, broad reflection between approximately 16 and 26 degrees two theta. This type of behavior is indicative of an amorphous, noncrystalline phase as opposed to opal (Hannington and Scott, 1988).

Backscattered electron (BSE) micrographs reveal the intricate textural nature of the siliceous clasts. The clasts are typically colloform, composed of interwoven, sub-micron size particles of silica of variable density. In a BSE micrograph (figure 4a), the layered nature of the clasts is apparent as differences in "grey level". In general, the denser portions of the silica clasts are brighter and the more porous portions are darker. However, many of the dark cores of the silica clasts seen in figure 4a are actually composed of stevensite, a tri-octahedral Mg-saponite. Stevensite forms the core of many of the siliceous clasts in both crust samples; stevensite is only found in the cores of the silica clasts and never within the rims or in the matrix of the crusts.

Many of the silica clasts contain small (<20 micron size) sulfide inclusions within their rims (figure 4a); these sulfides are dominantly pyrite/marcasite although locally chalcopyrite is abundant. In sample 769-1, a single, flat (approximately 1 square cm x 2 mm thick) clast of altered aphyric basalt was found. In this clast, the plagioclase is still unaltered, but the groundmass has been altered to Mg-silicate.

The porous matrix of the crusts is composed of (1) fine-grained amorphous silica, (2) bladed, acicular barite, and (3) disseminated clots of sulfide, dominantly marcasite, pyrite, and chalcopyrite, and rarer sphalerite (769-1). Rare microfossils are preserved in the matrix of these crusts: a silicified radiolarian (?) was found in 767-3 (figure 4b). Qualitative XRF analysis of a hydrothermal crust sample (769-1) reflects the mineralogy described above (figure 5). The dominant elemental constituents are Si (from amorphous silica and stevensite), Fe (from pyrite, marcasite, and chalcopyrite), Ba (from barite), S (from sulfides and barite), and Mg (stevensite). Subordinate constituents include Zn and Cu (from sulfides), Sr (from barite), and Al (from stevensite).

Chimney Fragments: Two samples from an active grey smoker spire were chosen for study: (1) a small (3.5 cm x 2.0 cm) dense, indurated fragment (769-3-D; figure 2c) and (2) highly friable, porous, and much less dense fragments (769-3-LD; figure 2d).

The dense fragment is texturally and mineralogically similar to the crust samples described above: it is clastic, although the sample is dominated by one large, subangular, white colored clast, nearly 1.5 cm in maximum dimension (right side, figure 2d). This heterogeneity of clast size is the main feature which distinguishes the dense chimney fragment from the two crust samples. The dense chimney fragment also contains an unusually large chalcopyrite grain (approximately 200 microns in maximum dimension) which is veined and rimmed by amorphous silica (figure 4c); the amorphous silica rim is itself rimmed by a fine grained, colloform aggregate of marcasite. Botryoidal clusters of marcasite, common in the matrix of the crusts, are also present in the matrix of 769-3-D. Such biogenically precipitated sulfide is rarely found in active chimneys (Robert Zierenberg, personal communication, 1989).

The less dense chimney fragments (769-3-LD) are both texturally and mineralogically distinct from the crust samples. This material is almost entirely composed of acicular, grey to white crystals of anhydrite (figure 2d), which readily disaggregate on handling. BSE micrographs (figure 4d) reveal that the anhydrite crystals (<5 mm in length) are locally rimmed by fibrous aggregates of a Mg-silicate phase, compositionally distinct from the stevensite described from the crust samples. These in turn are locally rimmed by or intergrown with fine grained aggregates of sphalerite, generally less than 10 microns in maximum dimension (figure 4d).

Basalt fragment: Sample 768-3 is a small fragment of debris collected within the active hydrothermal vent field. The fragment is a piece of fine-grained, aphyric basalt which contains a thin vein (< 1 mm) lined with layer silicates and pyrite crystals. As described below, microprobe analyses indicate that the layer silicate mineral is smectite-chlorite. The basalt is otherwise unaltered outside the vein. One other sample of basaltic material from within the vicinity of the vent field, 769-2, was also collected.

Petrographic examination of a small piece of this sample revealed no evidence for hydrothermal alteration in the interior of this sample.

Mineral chemistry

(1) Layer silicates: Three types of layer silicates were identified by electron microprobe analyses: (1) stevensite in the crust samples (769-1, 767-3) and dense chimney fragment (769-3D) (2) an as yet unidentified Mg-silicate in the less dense chimney fragment (769-3LD), and (3) smectite/chlorite in the basaltic debris fragment (768-3).

Analyses of layer silicates are presented in Table 2. Stevensites are nearly tri-octahedral smectites with total cationic sums approaching 14 on a 22 oxygen basis. The dominant octahedral cation is Mg, with Mg/22 oxygen ranging from 4.1 to 5.5 (figure 6a). The stevensites contain small, but significant quantities of Fe, Ca, Na, and K. Al₂O₃ varies from approximately 2.2 to 7.6 wt % (Table 2).

The unidentified layer silicate phase in the chimney fragment (769-3LD) is more Mg-rich than the stevensites (Table 2 and figure 6). Mg/22 oxygens average 7.5, far exceeding the maximum of 6.0 indicative of tri-octahedral smectites. This phase is also lower in Al₂O₃ and N₂O than the stevensite. Identification of this phase will require separation and detailed XRD study.

The vein filling layer silicates in the basalt fragment are more Al₂O₃ and FeO rich and SiO₂ poor than the stevensites (figure 6 and Table 2). Compositionally these minerals are interlayered mixtures of trioctahedral saponites and chlorites. The presence of smectite/chlorite as opposed to discrete smectite or chlorite implies that hydrothermal alteration of the basalt fragment occurred in the temperature range of approximately 150-250 degrees C (Bettison and Schiffman, 1988)

(2) Sulfides: Analyses of sulfides are presented in Table 3. Pyrites contain generally low amounts of Cu and Zn (<0.2 wt. %), but may contain up to 0.80 wt % As. Chalcopyrites are near end member in composition and contain negligible quantities of Zn or As. Sphalerites from the chimney fragment (769-3LD) are relatively Fe poor (< 3.5 wt. % Fe) and contain traces of Cu and Mn.

(3) Sulphates. Analyses of anhydrite and barite are presented in Table 4. Anhydrites from the chimney fragment (769-3L) are low in Ba and Sr. Barites from the crust samples and dense chimney fragment (769-3D) contain low Ca, but a large variation in Sr content (up to 6.8 wt % SrO). The Sr content of barite is inversely proportional to Ba content (figure 7).

Discussion

Grey Smoker Spires: The paragenesis of sphalerite-anhydrite-Mg-silicate found in the one studied sample (769-3) implies that the spires in the Seaciff hydrothermal field are of the low temperature (< 300 degrees C), "silica-sulfide-sulphate" variety, such as reported from the Axial Seamount caldera of the Juan de Fuca Ridge (Hannington and Scott, 1988). The abundance of amorphous silica and barite in the dense portion of the spire fragment (769-3D) argues for significant mixing of high temperature vent fluids with cold seawater and/or conductive cooling of

hydrothermal fluid beneath the spires. Further sampling is clearly required to adequately determine the petrogenesis of these spires.

Origin of hydrothermal crusts: The hydrothermal crusts from the Sea Cliff hydrothermal field are similar in many respects to the hydrothermal mound deposits reported from the Middle Valley of the Northern Juan de Fuca Ridge (Goodfellow and Blaise, 1988). In the Middle Valley region, the mound deposits are clastic mixtures of hydrothermally altered hemipelagic sediments and reworked exhalative chimney deposits, cemented by precipitation of amorphous silica and Mg-silicates from conductively cooled and mixed upwelling hydrothermal fluids.

In the Sea Cliff field, the crusts contain clasts of amorphous silica, commonly cored with stevensite. Several hypotheses could explain the origin of these clasts: (1) they are of originally pelagic or hemipelagic origin and have been mineralogically modified by reaction with hydrothermal fluid, (2) they are of basaltic origin and have been completely metasomatised by hydrothermal reaction, and (3) they are of entirely hydrothermal origin and represent direct precipitation of amorphous silica and stevensite from cooling hydrothermal fluids. The presence of rare radiolarian tests and basalt fragments in the crust samples lends some support to hypotheses 1 and 2. However, we have been unable to identify intermediate textural varieties between these possible parent materials and the silica-stevensite clasts; no evidence for hemipelagic (e.g., terrigenously derived) parent materials was found.

The close mineralogic and textural similarities of the crust and dense chimney samples argue for a hydrothermal origin for the crusts. The clasts could in part represent pieces of hydrothermal edifices which were subsequently broken and reworked. The anhydrite portions of the edifices would dissolve in cool seawater, leaving only the silica-sulfide-barite portions in the debris. Conversely, the crusts could have formed largely in situ by hydrothermal origin. In this scenario, stevensite (and minor sphalerite and chalcopyrite) form early from cooling hydrothermal fluids, upwelling diffusively away from the edifices. As the solutions cool, they precipitate amorphous silica which rims the stevensite. The clasts were locally reworked and mixed with minor biogenic and basaltic material. Hydrothermal activity continued and resulted in barite precipitation in pore spaces. A similar petrogenetic sequence has been proposed for hydrothermal mound deposits in the Guaymas Basin (Peter and Scott, 1988). Early stevensite deposition is believed to have occurred at temperatures between 300 and 250 C, and later amorphous silica and barite precipitation at temperatures below 250 C. Further work is warranted to more completely understand the petrogenesis of the Sea Cliff hydrothermal field crusts. In particular, it is important to determine the thickness of the crusts and the nature of their substrate.

Conclusions

The submersible observations, and the samples collected, largely support the hypothesis that hydrothermal circulation is accommodated, and perhaps controlled by faults. Even though no magma chamber is believed to exist under the Sea Cliff Hydrothermal Field, the faults apparently allow penetration into the hot lower crust or upper mantle.

The full extent of the hydrothermal field is not known, nor is the quantity of hydrothermal products. In particular the volume of sulfides cannot yet be estimated. The mineralogy of the samples we have collected implies that the field has had a complicated history. The difference between the fossil chimneys and those presently active suggests that mineral deposition may have changed during the life of the field, and perhaps during the lives of specific vents. Additional work, and additional samples are needed to unravel the history.

For the purposes of the Gorda Ridge Technical Task Force, perhaps the most important result of this study is that we have shown that future minerals exploration should not be restricted to the axis of the ridge on the rift valley floor. Instead, the rift valley walls must also be explored.

References Cited

- Bettison, L.A. and Schiffman P. (1988) Compositional and structural variations of phyllosilicates from the Point Sal ophiolite, California. *American Mineralogist* 73, 62-76.
- Goodfellow, W.D. and Blaise, B. (1988) Sulfide formation and hydrothermal alteration of hemipelagic sediment in Middle Valley, northern Juan de Fuca Ridge. *Canadian Mineralogist* 26, 765-696.
- Hannington, M.D. and Scott, S.D. (1988) Mineralogy and geochemistry of a hydrothermal silica-sulfide-sulfate spire in the caldera of Axial Seamount, Juan de Fuca Ridge. *Canadian Mineralogist* 26, 603-625.
- Peter, J.M. and Scott, S.D. (1988) Mineralogy, composition, and fluid-inclusion microthermometry of seafloor hydrothermal deposits in the southern trough of Guaymas Basin, Gulf of California. *Canadian Mineralogist* 26, 567-587.
- Rona, P.A., & D.A. Clague, (1989) Geologic controls of hydrothermal discharge on the northern Gorda Ridge, manuscript submitted.
- Rona, P.A., R. Denlinger, M. Fisk, K. Howard, K. Klitgord, J. McClain, G. McMurray, G. Taghon, J. Wiltshire, (1989) Sea Cliff Hydrothermal Field on the northern Gorda Ridge, abstract submitted, manuscript in preparation.

Figure Captions

1. Geologic map of the Seacliff hydrothermal field. (b) Locations of samples analyzed in this study.
2. Photographs of hydrothermal crust and chimney samples. (a) 767-3; (b) 769-1; (c) 769-3D; (d) 769-3LD. Scale bar in all photos = 1 centimeter.
3. X-ray diffraction powder pattern of crust sample 769-1. The broad reflection between approximately 15 and 26 degrees 2 theta (Cu Ka radiation) is indicative of amorphous silica. The small peaks above 21 degrees are barite reflections.
4. Backscattered electron micrographs of crust and chimney samples. (a) 769-1: colloform amorphous silica clasts cored by stevensite; the porous matrix is composed of amorphous silica, bladed barite, and sulfide (small bright clots); scale bar = 0.5 mm. (b) 767-3: radiolarian (?) test in fine grained siliceous matrix of hydrothermal crust; scale bar = 0.2 mm. (c) 769-3D: chalcopyrite veined and rimmed by amorphous silica, in turn rimmed by fine-grained marcasite; matrix is composed of amorphous silica, sulfides, and barite; scale bar = 0.1 mm. (d) 769-3LD; anhydrite rimmed by fibrous Mg-silicate, in turn rimmed by fine grained sphalerite (bottom); scale bar = 0.2 mm.
5. Qualitative XRF analyses of crust sample 769-1. (a) analysis by direct excitation with the Rh X-ray tube; (b) analysis with a Ge secondary fluorescence target; (c) analysis with a Rh fluorescence target.
6. Electron microprobe analysis of layer silicates. (Top) Si versus Mg; (Bottom) Total cations versus Al; all cationic proportions on the basis of 22 oxygens. Symbols; open squares = stevensite in crusts, filled square = Mg-silicate in 769-3LD, filled triangles = smectite/chlorite in basaltic fragment 768-3.
7. Sr versus Ba contents of barites. Symbols; open square = 769-3D; filled square = 769-1; open triangle = 767-3.

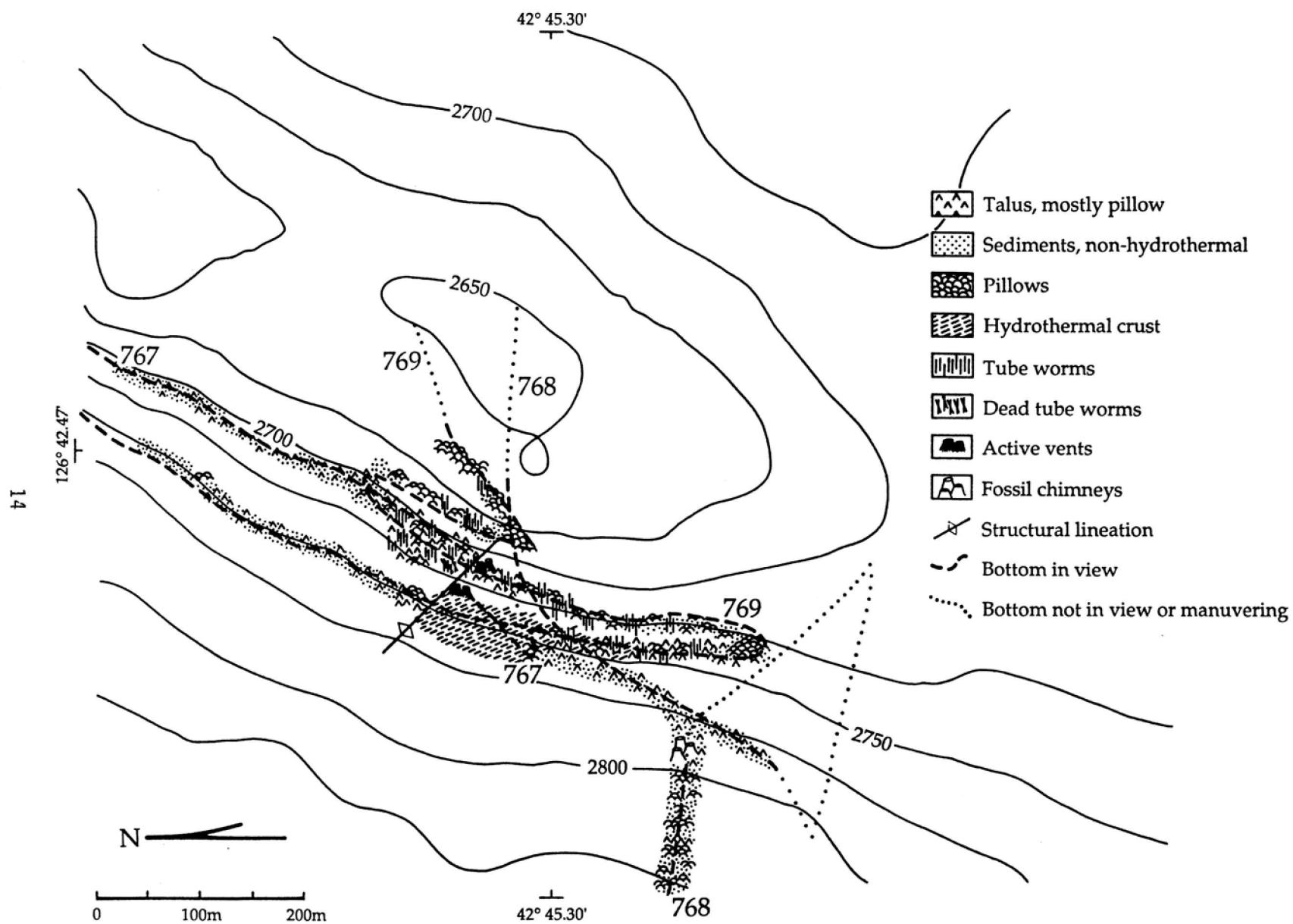


Figure 1a

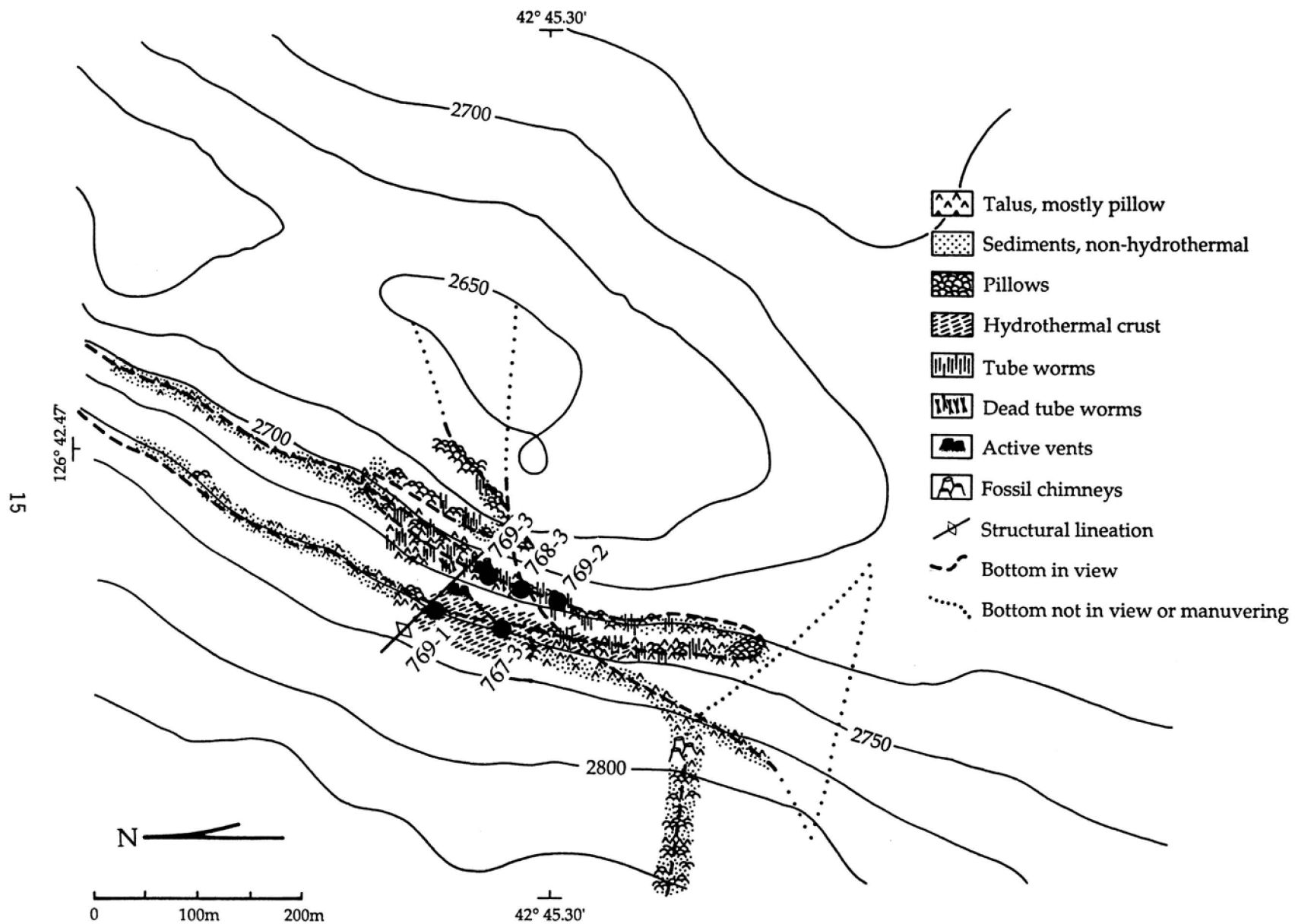


Figure 1b

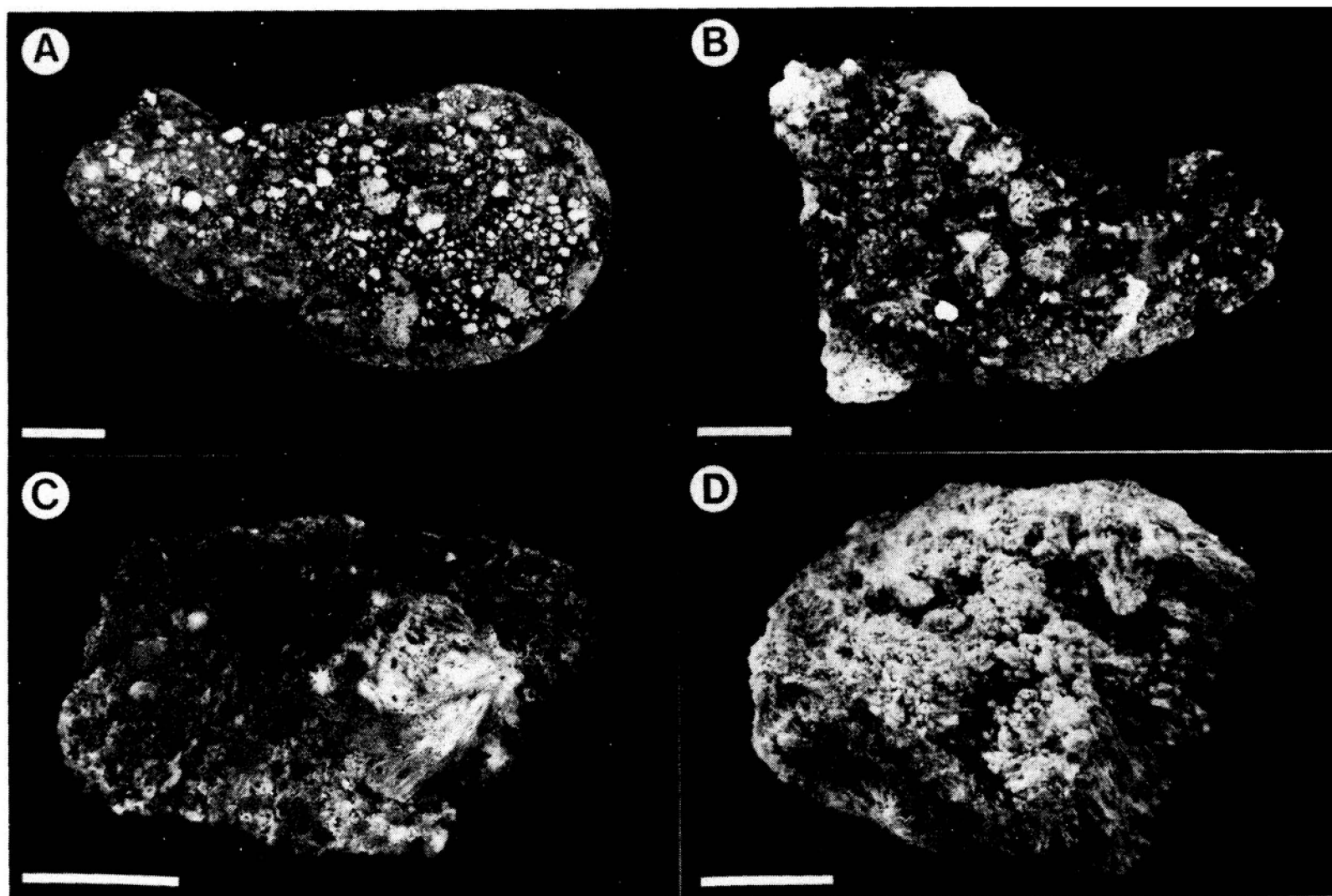


FIGURE 2

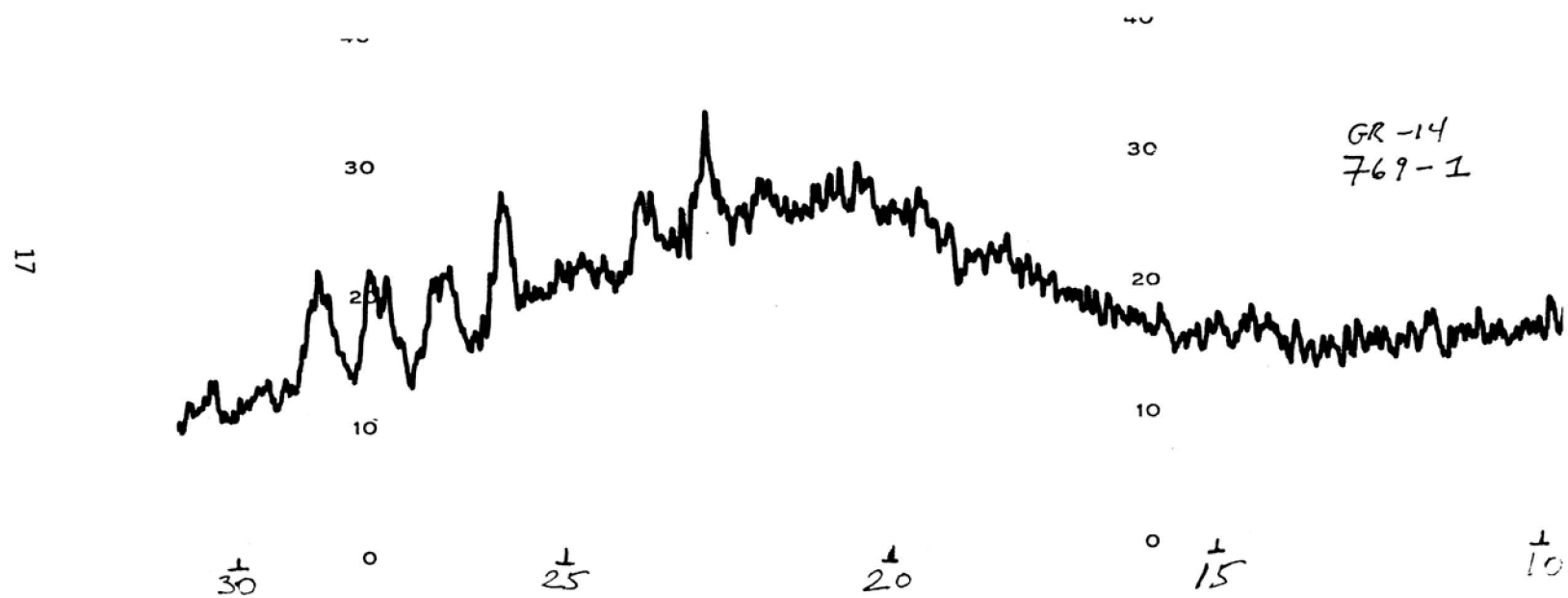


Figure 3

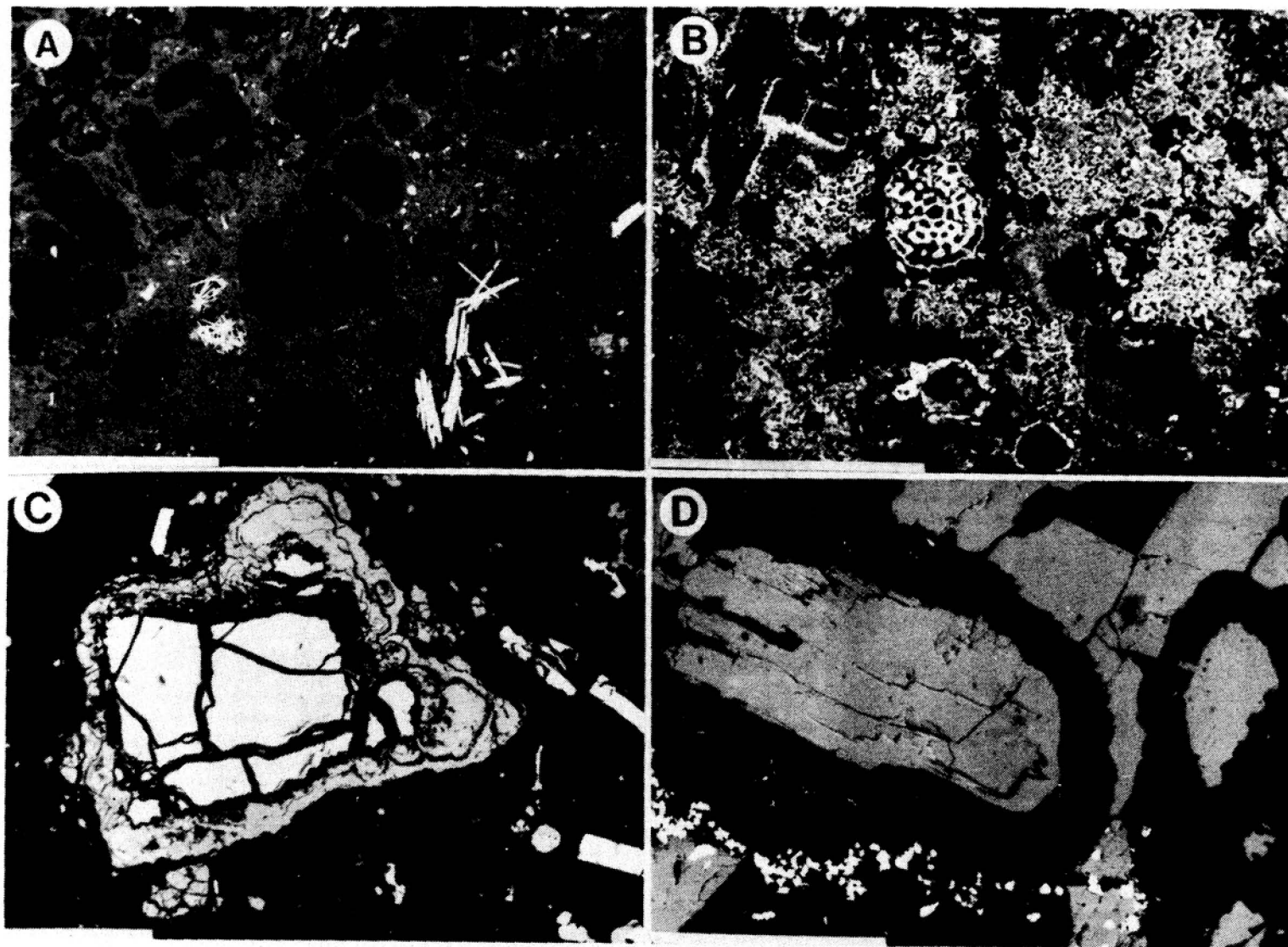


Figure 4

25-Nov-1988 18:14:18

GORDA RIDGE 14

769-1 DIRECT EXCITATION (RH TUBE)

Preset= 200 secs

Vert= 2000 counts Disp= 1 Comp= 2 Elapsed= 69 secs

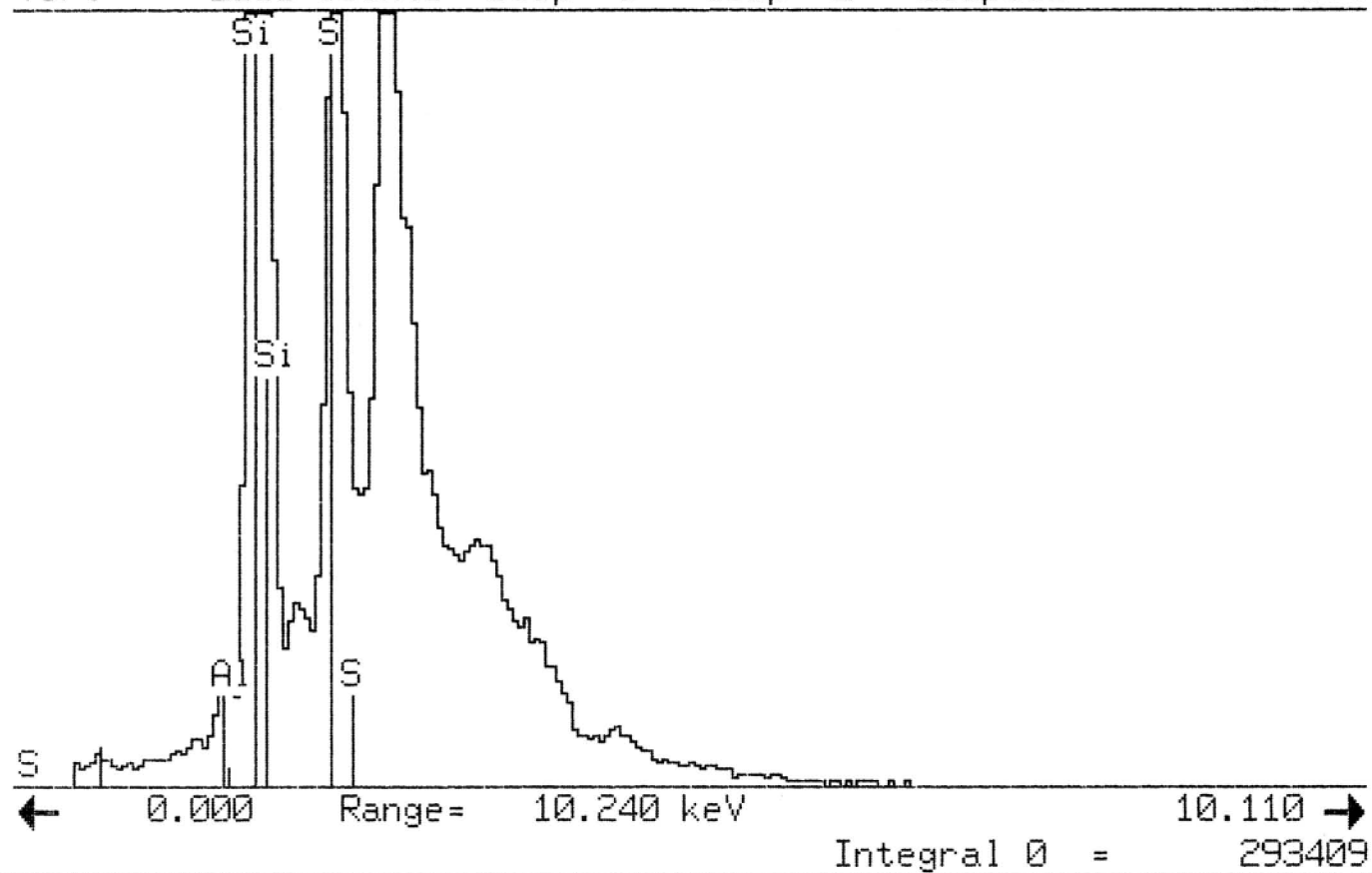


Figure 5A

25-Nov-1988 17:54:27

GORDA RIDGE GR 14

769-1 GE TARGET ANALYSIS

Vert= 3489 counts Disp= 1 Comp= 2 Elapsed= 103 secs

A1= 1 P1= 1 P2= 2

Preset= 200 secs

Elapsed= 103 secs

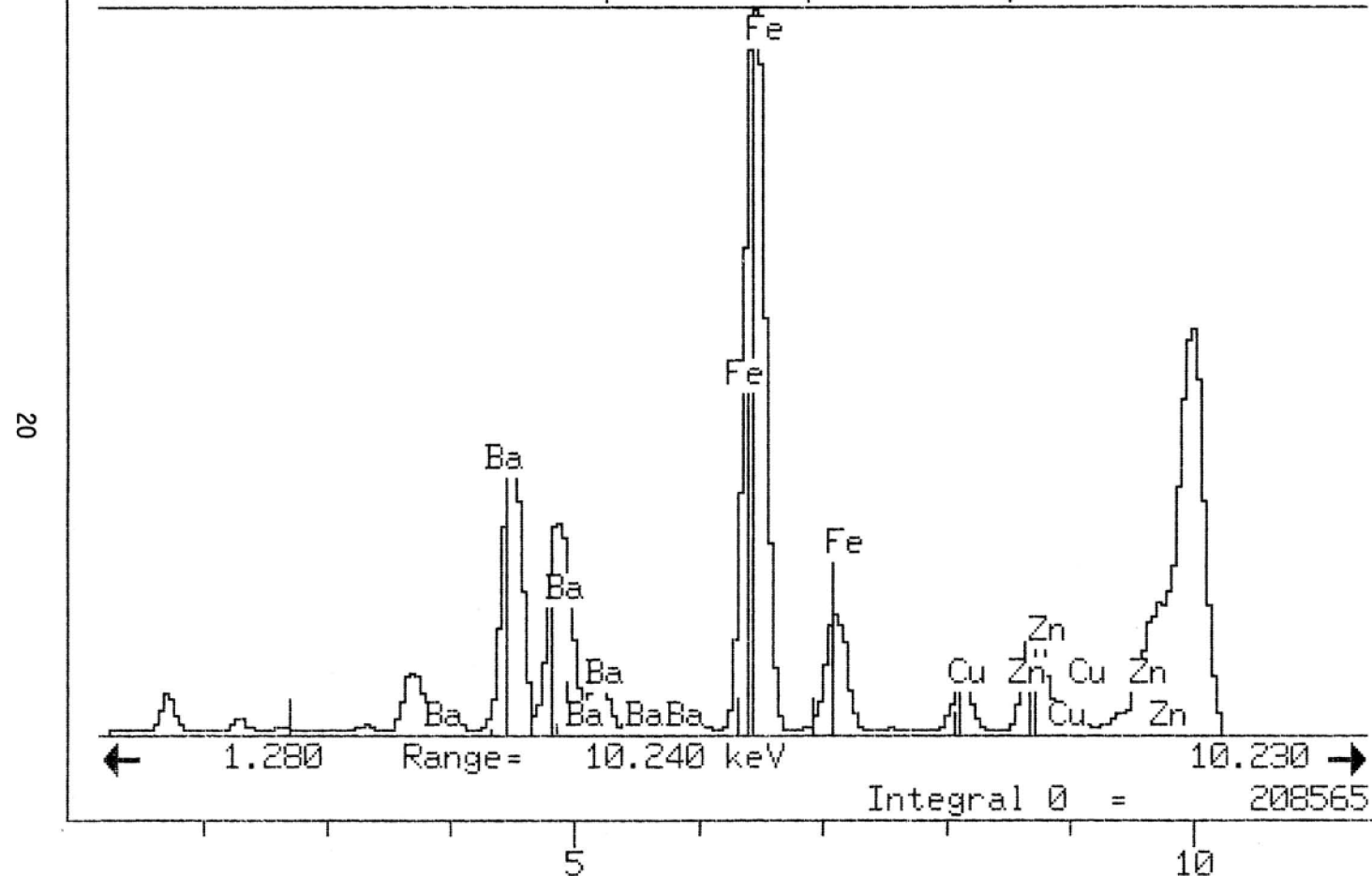


Figure 5B

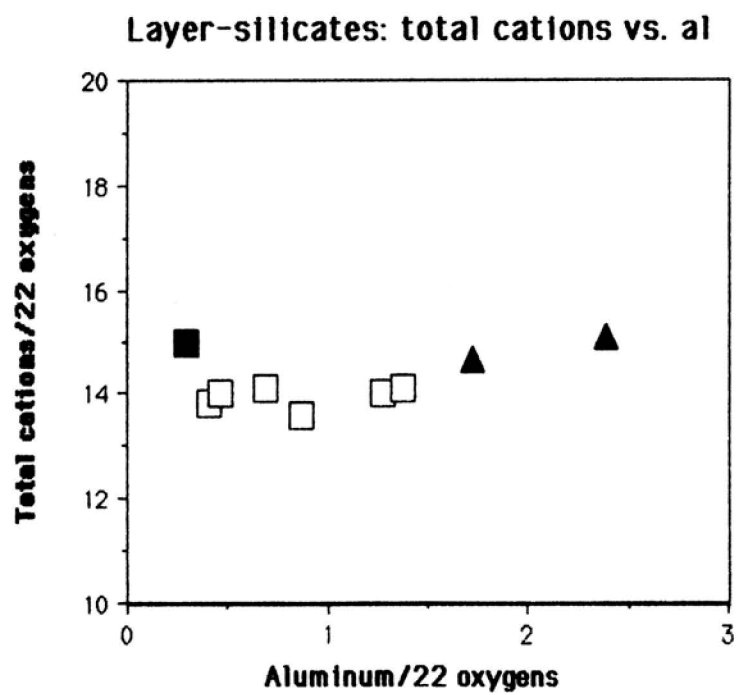
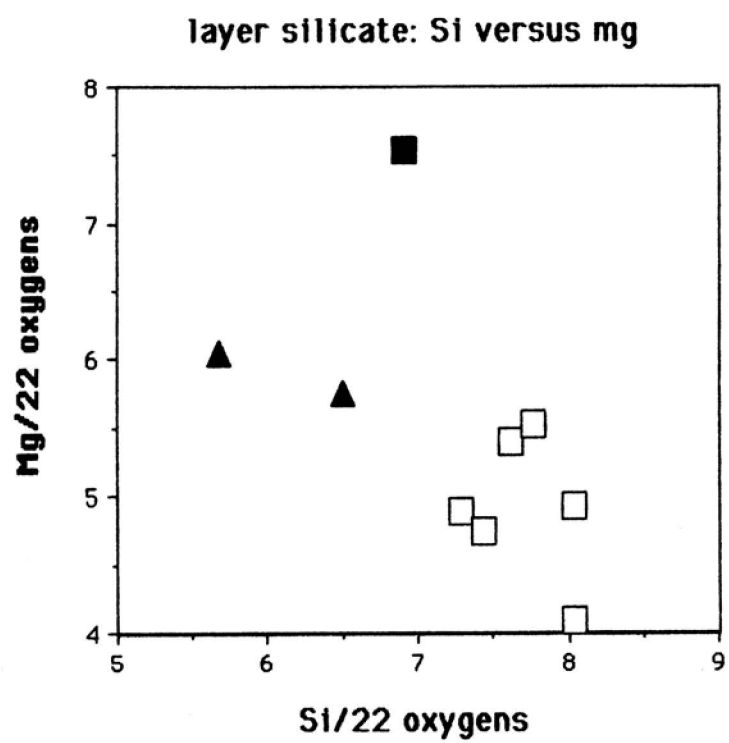


Figure 6

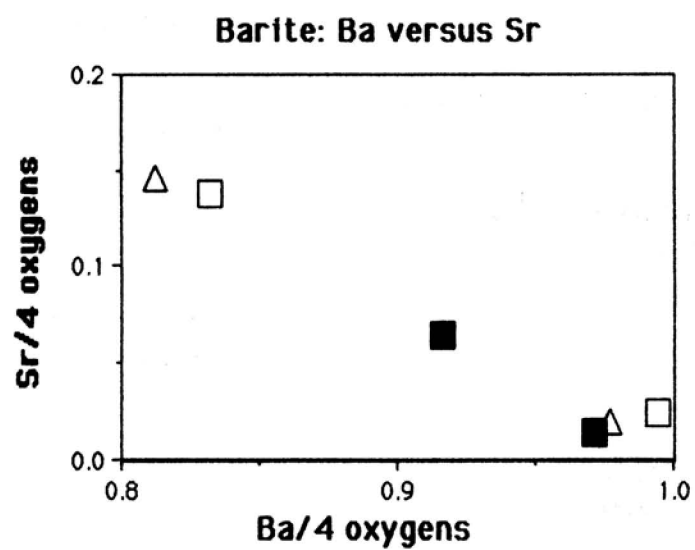


FIGURE 7

TABLE 1
SAMPLES ANALYZED IN THIS STUDY

SAMPLE #	DESCRIPTION	SIZE(CM)	HYDROTHERMAL MINERALOGY
767-3	Hydrothermal crust	14x7x3	amorphous silica barite stevensite pyrite/marcasite chalcopyrite
768-3	Basaltic fragment	2.5x2.2x1	pyrite smectite/chlorite
769-1	Hydrothermal crust	11x14x4.5	amorphous silica barite stevensite pyrite/marcasite chalcopyrite sphalerite
769-3 D	Chimney fragment from grey smoker spire (dense portion)		amorphous silica barite stevensite pyrite/marcasite chalcopyrite sphalerite
769-3 LD	Chimney fragment from grey smoker spire (less dense portion)		anhydrite sphalerite Mg-silicate

TABLE 2

**SEACLIFF HYDROTHERMAL FIELD
LAYER SILICATES
(22 OXYGENS)**

	769-1	769-1	767-3	767-3	769-3LD	769-3D	769-3D	768-3	768-3
SiO ₂	47.14	48.72	47.79	53.83	48.34	50.69	51.75	37.65	44.81
TiO ₂	0.05	0.17	0.01	0.02	0.00	0.00	0.01	0.78	0.03
Al ₂ O ₃	7.61	7.12	3.70	2.71	1.69	2.19	4.74	13.43	10.06
MgO	21.29	20.84	22.83	25.74	35.36	20.83	17.67	26.91	26.51
CaO	0.65	0.50	0.29	0.34	0.23	0.12	0.48	0.32	0.80
MnO	0.07	0.05	0.03	0.02	0.10	0.17	0.03	0.05	0.05
FeO	1.77	1.94	1.48	1.14	1.04	1.97	2.66	6.13	3.70
Na ₂ O	0.36	0.28	0.41	0.17	0.07	0.25	0.29	0.06	0.23
K ₂ O	0.51	0.43	0.16	0.16	0.24	0.38	0.40	0.10	0.15
Total Oxides	79.45	80.05	76.70	84.13	87.07	76.60	78.03	85.43	86.34
Si	7.28	7.44	7.61	7.77	6.91	8.04	8.04	5.67	6.51
Ti	0.01	0.02	0.00	0.00	0.00	0.00	0.00	0.09	0.00
Al	1.38	1.28	0.69	0.46	0.29	0.41	0.87	2.39	1.72
Mg	4.90	4.74	5.41	5.54	7.54	4.93	4.09	6.04	5.75
Ca	0.11	0.08	0.05	0.05	0.04	0.02	0.08	0.06	0.13
Mn	0.01	0.01	0.01	0.00	0.01	0.02	0.00	0.01	0.01
Fe	0.23	0.25	0.20	0.14	0.12	0.26	0.35	0.77	0.45
Na	0.11	0.09	0.13	0.05	0.02	0.08	0.09	0.02	0.06
K	0.10	0.09	0.03	0.03	0.04	0.08	0.08	0.02	0.03
Total Cations	14.13	14.00	14.13	14.04	14.97	13.84	13.60	15.05	14.66

TABLE 3

**SEACLIFF HYDROTHERMAL FIELD
SULFIDES**

	Sphalerite	Chalcopyrite				Pyrite	
	769-3 L	769-3 D	767-3	769-1	769-3 D	767-3	769-1
S	32.91	34.82	34.27	34.33	53.20	53.32	52.63
Mn	.11	.01	.04	.00	.00	.00	.02
Fe	3.22	30.69	30.01	30.11	45.35	46.65	46.18
Cu	.21	33.98	34.21	34.39	.17	.04	.11
Zn	63.88	.03	.00	.03	.07	.00	.03
As	.00	.03	.00	.02	.32	.07	.80
Total	100.33	99.56	98.53	98.88	99.10	100.08	99.78
S	.497	.500	.498	.498	.669	.665	.661
Mn	.009	.000	.000	.000	.000	.000	.000
Fe	.028	.256	.250	.251	.328	.334	.332
Cu	.002	.246	.251	.252	.001	.000	.000
Zn	.473	.000	.000	.000	.000	.000	.000
As	.000	.000	.000	.000	.002	.000	.004

TABLE 4

**SEACLIFF HYDROTHERMAL FIELD
SULPHATES
(4 OXYGENS)**

	Anhydrite			Barite			
	<u>769-3 LD</u>	<u>769-3 D</u>	<u>769-3 D</u>	<u>767-3</u>	<u>767-3</u>	<u>769-1</u>	<u>769-1</u>
S03	57.75	33.78	36.08	34.38	36.20	34.44	34.80
CaO	40.73	.04	.44	.04	.81	.22	.07
SrO	.27	1.11	6.41	.83	6.83	.63	2.88
BaO	.06	64.80	57.21	64.26	56.09	63.91	60.69
Total	98.81	99.73	100.14	99.51	99.93	99.20	98.44
S	.997	.993	1.004	1.001	1.003	1.002	1.006
Ca	1.004	.001	.017	.002	.032	.009	.003
Sr	.003	.025	.138	.019	.146	.014	.064
Ba	.001	.994	.832	.977	.812	.971	.916
Total	2.005	2.013	1.991	1.999	1.993	1.996	1.989